Digitally Assisted Analog Mitigation of Narrowband Periodic Interference

Karel Pärlin* and Taneli Riihonen†
*Rantelon, Tallinn, Estonia
†Electrical Engineering, Tampere University, Finland
e-mail: karel.parlin@rantelon.ee, taneli.riihonen@tuni.fi

***Abstract*—Interference mitigation in radio-frequency (RF) receivers has been studied extensively in various contexts. And although most of the in-band interference mitigation techniques rely on suppressing the interference in the digital domain, strong in-band interference can saturate a receiver's front-end and, thus, prevent it from receiving comparatively weak signals of interest. This is especially so in case of the self-interference (SI) encountered in enclosed full-duplex (FD) radios, but also in case of co-located jammers or radars and signals intelligence receivers. This work presents a digitally assisted method and its implementation for the mitigation of narrowband periodic interference before quantization in order to improve the sensitivity of receivers co-located with strong interference sources. Experimental results are provided and the potential for mitigating more complex waveforms, e.g., pseudorandom jamming, is discussed.**

I. Introduction

Impelled by the threat of adversarial jamming and the increased congestion of the radio-frequency (RF) spectrum, the mitigation of in-band interference in RF receivers has received considerable attention in defense and security research. Based on their usage domain, the mitigation techniques fall into two categories. Digital interference mitigation can be sufficient against adversarial jamming [1], whereas high-power interference from co-located transmitters can lead to adjusting the receiver's analog-to-digital converter (ADC) range to prevent overloading. Thus, the receiver would benefit from suppressing the interference in the analog domain before quantization to improve the effective resolution of the signal of interest [2].

The interference problem encountered in the case of co-located transmitters and receivers is similar to the self-interference (SI) challenge in full-duplex (FD) radios that operate in same-frequency simultaneous transmit and receive (SF-STAR) mode [3]. Such operation is expected to increase the spectral efficiency in wireless communications but SF-STAR has also been envisioned to reshape both the wireless defense and security domains, e.g., in the form a so-called FD radio shield [4]. Inside the radio shield, a central node would be capable of receiving wireless signals while jamming the reception of those or other malign signals for others. The concept can be further elaborated to include pseudorandom jamming signals, which the authorized users inside the FD radio shield can suppress. This again potentially raises the receiver overloading issue.

This research work was partly supported by the Academy of Finland under the grant 315858 "Radio Shield Against Malign Wireless Communication."

The aim of this work is to develop a method for mitigating narrowband interference in receivers co-located with high power transmitters as envisioned in Fig. 1, i.e., without having direct access to a copy of the interfering transmission as opposed to FD radios. We propose a digitally assisted analog interference cancellation technique using a single input antenna and adaptive filtering by extending our previous work on digital cancellation [5]. Experimental results characterize the performance of the proposed method in a laboratory environment and reveal that phase noise, which in the case of FD radios with a shared local oscillator (LO) is inherently mitigated [6], is one of the main limiting factors for interference mitigation. With co-located devices, sharing the LO can be impractical, otherwise the interfering signal could also be shared to simplify its mitigation.

The remainder of this paper is organized as follows. In Section II, the interference mitigation technique is introduced. The experimental setup that was used assess this method is discussed in Section III and the results are presented in Section IV. Finally, the paper is concluded in Section V.

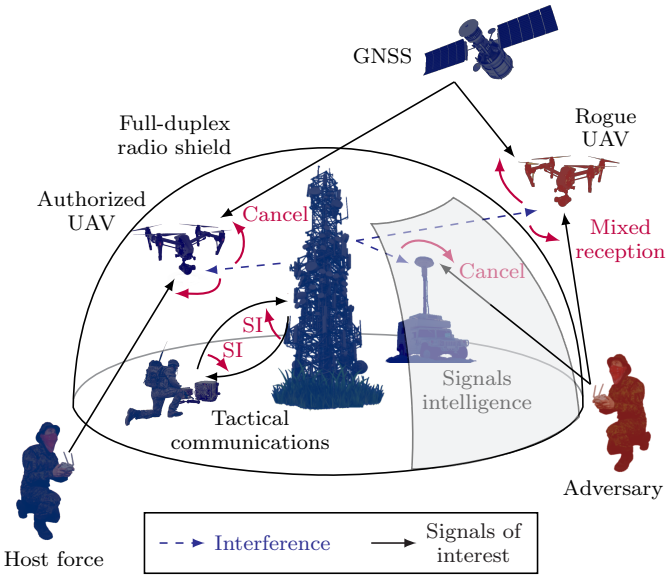

Fig. 1. The mitigation of co-located interference facilitates, e.g., the remote control of unmanned aerial vehicles (UAVs), the reception of global navigation satellite system (GNSS) signals, tactical wireless communications, and many other radio systems in the electronic battlefield as well as in civilian security.

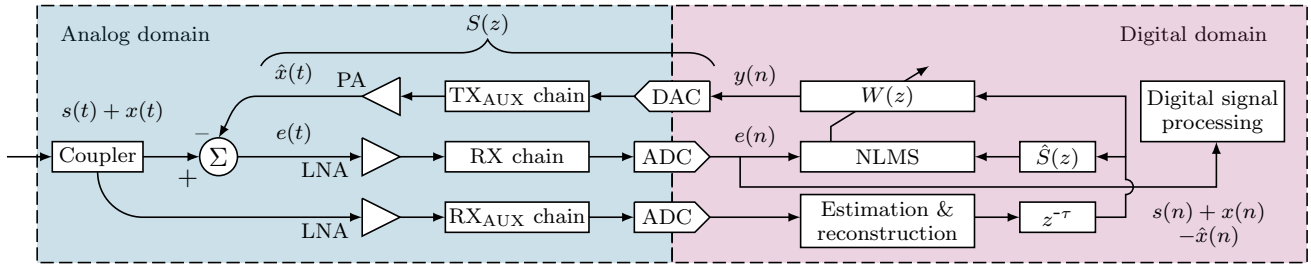

Fig. 2. Digitally assisted analog mitigation of instantaneously narrowband periodic interference based on adaptive filtering.

II. Narrowband Interference Mitigation

The mitigation of co-located interference in the analog domain prior to digitization offers an opportunity to improve the receiver sensitivity of co-located radios [7]–[9]. This section briefly analyzes the circumstances under which analog interference mitigation becomes necessary and proposes a digitally assisted analog interference mitigation technique (Fig. 2).

A. SINR Analysis

As the receiver's automatic gain control (AGC) keeps the total ADC input at constant full range level, high interference power means more ADC dynamic range is consumed by the interference signal. This leads to reduced effective resolution for the signal of interest, which may limit the receiver's performance [10]. The signal-to-interference-plus-noise ratio (SINR) can be calculated [11] as follows:

$$\gamma = \frac{\rho}{\frac{P_S L_S}{P_I L_I/\Delta_a} + \rho/\Delta_d + 1} \cdot \frac{P_S L_S}{P_I L_I/\Delta_a}, \tag{1}$$

where $P_S L_S/(P_I L_I/\Delta_a)$ represents SINR after path losses and analog cancellation, ρ is the effective dynamic range, and Δ_d is the amount of digital cancellation. Whether or not digital cancellation is sufficient depends on the targeted SINR γ_t of the application. The minimal level of digital suppression needed to achieve $\gamma \geq \gamma_t$ given $P_S L_S/P_I L_I$, Δ_a, and ρ can be solved from (1) as

$$\Delta_d \geq \frac{\rho}{\frac{P_S L_S}{P_I L_I/\Delta_a} \cdot (\frac{\rho}{\gamma_t} - 1) - 1}, \tag{2}$$

if $\Delta_a \cdot \frac{P_S L_S}{P_I L_I} \geq \frac{\gamma_t}{\rho}$, otherwise the target SINR cannot be achieved regardless of the level of digital suppression [11].

Taking free-space path loss into account and assuming no analog cancellation, Fig. 3 illustrates the maximum attainable SINR after ideal digital interference cancellation ($\Delta_d = \rho$) in terms of distances between the transmitters of the signals of interest TX_S and interference TX_I from the receiver RX. The output power ratio between the transmitters is taken to be $P_S/P_I = -23$ dB and the effective dynamic range of the receiver is assumed to be $\rho = 48$ dB, corresponding to a 12-bit ADC with effective number of bits (ENOB) equalling 10 [3]. The calculated results illustrate the extent to which a co-located transmitter limits the receiver's sensitivity if only digital interference mitigation is used.

B. Digitally Assisted Analog Interference Mitigation

Expanding on our previous work in digital narrowband interference mitigation, which relies on estimating the instantaneous frequency of the strong interfering signal, reconstructing such a signal, and using adaptive filtering to suppress the interference [5], we propose to use an auxiliary transmit chain to subtract the reconstructed, delayed, and filtered interference from the received signal in the analog domain as illustrated in Fig. 2. Similar methods have been successfully applied in FD radio prototypes to cancel the SI [12], in adaptive noise control (ANC) to suppress acoustic noise by introducing "antinoise" of equal amplitude and opposite phase [13], and have also been considered in theory for evading radars by cancelling their echoes [14]. However, this work combines RF interference estimation and its mitigation before quantization and provides experimental results.

The proposed method is based on the estimating the instantaneous frequency of the narrowband jamming signal $x(n)$ and constructing a digital representation $\hat{x}(n)$ of the jamming signal such that it exactly follows the estimated frequencies. As previously shown in [5], it is possible to estimate the instantaneous frequency of narrowband interference as long as

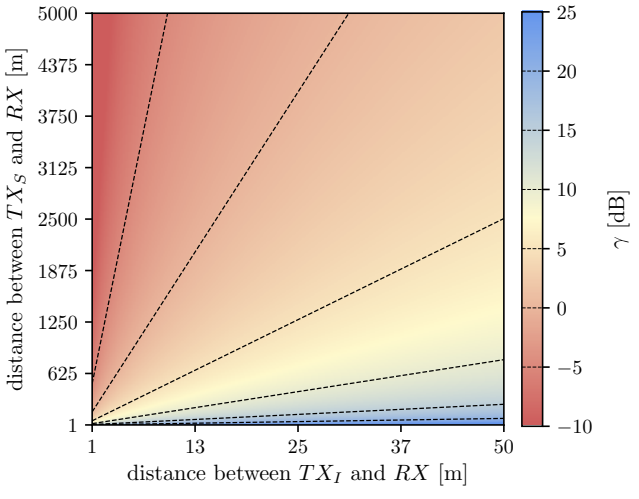

Fig. 3. The maximum attainable SINR in terms of distances between the transmitters of the desired and interfering signals and the receiver. Assuming no analog interference mitigation and ideal digital interference mitigation. Here $P_S/P_I = -23$ dB and only free-space path loss is considered.

the interference is sufficiently more powerful than the signal of interest. In order to obtain an interference-free version of $s(n)$, the clean input signal corrupted by interference $s(n)+x(n)$ is employed as the reference signal for the adaptive filter, whose input is the estimated jamming signal $\hat{x}(n)$ that is strongly correlated to the actual jamming signal $x(n)$. The adaptive mechanism adjusts the filter coefficients of $W(z)$ in such a manner that the filter output $y(n)$ approximates the jamming signal $x(n)$, thus forcing the error signal $e(n)$ to resemble the signal of interest $s(n)$. The system uses a directional coupler to direct some of the input signal energy to a secondary receiver port RX_{AUX} that is not affected by the cancellation and thus allows to continue estimating the interfering signal simultaneously to its mitigation in the primary path RX.

Unfortunately, the digital interference reconstruction takes a considerable amount of time and consequently the computational delay in generating the $\hat{x}(n)$ becomes longer than the path delay in the primary receiver chain for the actual interference $x(n)$. Therefore, the system's response is noncausal and the system is capable of effectively canceling only narrowband or periodic interference [13]. Furthermore, for the interference estimation, the actual signals of interest act as noise.

Compared to digital interference mitigation, the use of adaptive filtering for analog interference mitigation is further complicated by the fact that the summation of signals represents RF superposition and it is necessary to compensate for the secondary-path transfer function $S(z)$, which includes the digital-to-analog converter (DAC), TX_{AUX} chain, power amplifier (PA), power combiner, low-noise amplifier (LNA), RX chain, and ADC. Thus, the purely digital adaptive filter based on the normalized least mean squares (LMS) algorithm is extended to a filtered-x version, where a transfer function is present in the cancellation path.

The filtered-x least mean squares (FxLMS), however, becomes unstable at step sizes much lower than without the secondary path, thus limiting the convergence speed [15]. That is because the secondary path influences the dynamic response of the cancellation system by reducing the maximum step size in the FxLMS algorithm. On the other hand, the FxLMS algorithm is rather tolerant to errors made in the estimation of $S(z)$ by the filter $\hat{S}(z)$, as within the limit of slow adaptation, the algorithm converges with nearly 90° of phase error between $S(z)$ and $\hat{S}(z)$ [13]. Therefore, offline modeling can be used to estimate $S(z)$ during an initial training stage as the signal path from the auxiliary transmitter TX_{AUX} to the primary receiver RX can be considered static.

A single-frequency reference based adaptive canceller using the LMS algorithm has the properties of a notch filter at the reference frequency and the level of interference is reduced at the expense of introducing some distortion on the desired signal [16]. The same applies to the FxLMS with an intervening transfer function in the cancellation path [15]. The system in general can possibly be repurposed to work with broadband interference, such as pseudorandom jamming, e.g., by replacing the narrowband interference reconstruction with a respective signal generator.

III. Experimental Setup

In order to characterize the performance of the proposed RF interference mitigation technique, we carried out experiments in a laboratory environment. The experimental setup as illustrated in Fig. 4 simulates a scenario, in which a co-located jammer is interfering with a receiver, omitting any signals of interest. All the devices involved in the measurements were connected through coaxial cables, thus providing a controlled environment in which all other sources of interference, besides the devices under test, were eliminated. This also ensured precise control of the power levels during the measurements. Furthermore, effects in the radio channel, such as multipath propagation and fading, do not have an effect on the measurement results and a wide frequency range from 100 MHz to 2400 MHz could be studied without restrictions.

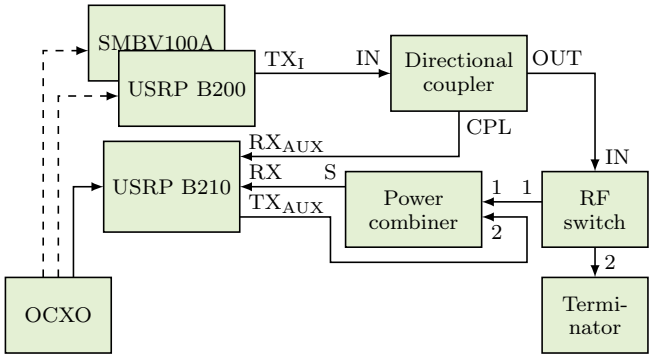

Fig. 4. The measurement setup in which either the SMBV100A vector signal generator or the USRP B200 software-defined radio is used to generate the interference. An oven-controlled crystal oscillator (OCXO) is used as an external reference either for the receiver only or for both the interference generator and the receiver.

A. Experimental Receiver

The receiver prototype used in the measurements is built using the USRP B210 commercial off-the-self (COTS) dual-channel software-defined radio (SDR) that receives signals in a 2 MHz bandwidth. In order to improve its phase noise characteristics, a 10 MHz oven-controlled crystal oscillator (OCXO) based reference clock is used as an external reference. Furthermore, in order to examine the effect of using a shared reference clock for both the receiver and the interference generator, as is typically the case in FD radios, measurements were carried out by using the OCXO as reference for only the receiver or both the receiver and the interference generator.

The input signal, i.e., the interference, is split in two using a directional coupler and a wideband electromechanical RF switch is used to control the input signal flow into the primary receiver path RX. This allows to carry out offline secondary path modelling during an initial training stage. A two-way power combiner is used to combine the received signal and the generated cancellation signal. The resulting signal path from the interference generator's TX_I to the receiver's RX attenuates the signal by 5 dB to 8 dB in the frequency range of 100 MHz to 2400 MHz.

B. Interference

The interference was generated at center frequencies of 100, 200, 400, 800, 1600, and 2400 MHz with two different methods. Using a Rohde & Schwarz vector signal generator SMBV100A and using an Ettus USRP B200 SDR. Also two different kind of interference were used, a single-tone signal and a sinusoidally frequency-modulated (FM) signal with frequency deviation of 125 kHz and modulation rate of 1 kHz. The frequency deviation and modulation rate were chosen based on the limitations imposed by the SMBV100A at 100 MHz and applied at all of the measured center frequencies with both interference generators. In either case the interference is instantaneously narrowband and periodic. The interference power was limited to -20 dBm, which is close to the specified maximum input level of the USRP B210.

IV. Experimental Results

The interference cancellation results, i.e., the measured power reduction after cancellation, over the examined frequency range for both single-tone and FM interference are plotted in Fig. 5. The vector signal generator has considerably lower phase noise of the two tested interference sources, which explains the better efficiency of the interference cancellation. Specifically, the AD9364 transceiver chip used in the USRP B200 has specified integrated phase jitter of 58.9 ps at 2400 MHz, whereas the SMBV100A has phase jitter of only 3.9 ps at 1000 MHz. The single-tone interference cancellation results are thus in agreement with the active cancellation studies with regards to the variance of phase noise in FD radios with non-matched LOs [17].

Furthermore, the interference cancellation results demonstrate an exponential dependence on the center frequency. This is also explained by the differences in phase noise. Ideally, frequency multiplication by N results in phase noise increase by $20 \cdot \log_{10} N$, i.e., 6 dB in the case of frequency doubling. Measurement results for the single-tone interference cancellation are consistent with the 6 dB per octave performance degradation. In the case of FM interference, the maximum achievable suppression rate is further limited by the frequency stability of the FM source and by the ability of the interference mitigation system to exactly estimate and regenerate the periodic interference.

From the results, it also becomes evident that sharing a common external reference between the interference generator and the interference mitigating receiver improves the active cancellation efficiency. This is in accordance with the studies on phase noise effects in FD radios, whereas sharing the LO between the transmit and receive chains inherently mitigates the performance hampering effect of phase noise. These results stress the importance of using high-precision oscillators in co-located radios in order to lower the phase noise and achieve efficient interference cancellation. When considering the mitigation of broadband or pseudorandom interference, the jamming waveforms could perhaps be designed to facilitate digital estimation and suppression of phase noise likewise to recent advances in FD radios [18].

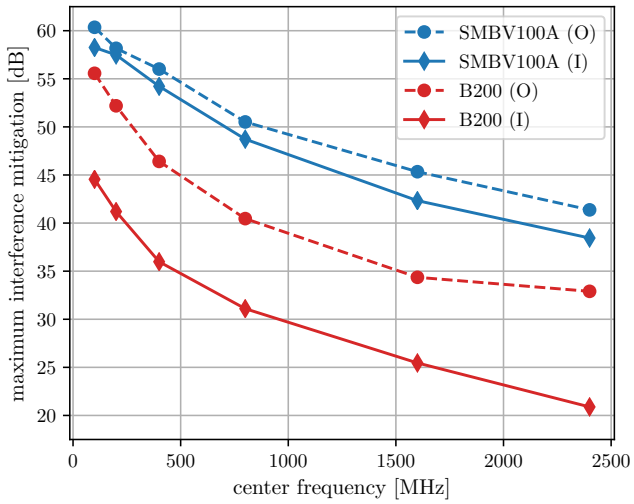

(a) under single-tone interference

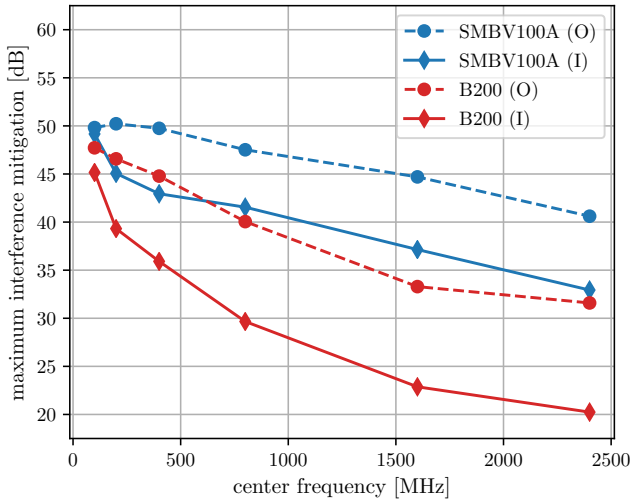

(b) under sinusoidally frequency-modulated interference

Fig. 5. Analog interference mitigation achieved in the 100 MHz to 2400 MHz frequency range using the different measurement setup configurations. The interference generator was referenced either by its internal clock (I) or the oven-controlled crystal oscillator based external reference clock (O), which was also used as an external reference for the receiver.

Another important aspect of adaptive filtering is the learning rate by which the interference can be cancelled. The learning rate of the analog RF interference cancellation for single-tone and FM interference is visualized in Fig. 6. For the single-tone interference, the adaptive filter converges in approximately 100 µs, whereas for the FM interference, the filter converges typically in a matter of seconds. Furthermore, such predictive interference cancellation method inherently produces a short burst of interference by itself when the actual interference in the input signal disappears. All of the measurements were made with a small step size that was empirically found to be close to (but still below) the upper bound beyond which the adaptive filter becomes unstable. As mentioned previously, this is affected by the imposed delay of the secondary path.

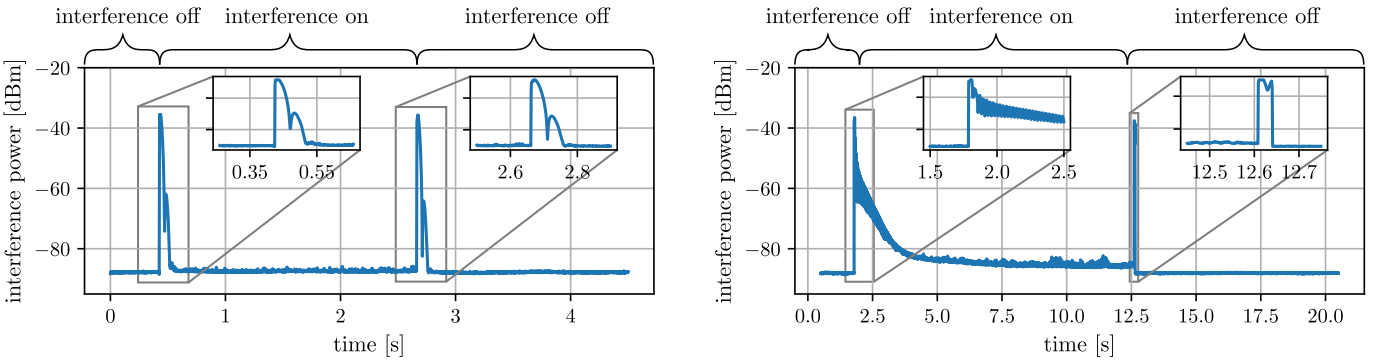

(a) under single-tone interference

(b) under sinusoidally frequency-modulated interference

Fig. 6. Learning curves of the adaptive digitally assisted analog radio-frequency interference mitigation system as measured for a single-tone and a sinusoidally frequency-modulated interference in a closed and static laboratory environment. Whenever no interference is present the system reaches noise level of -88 dBm.

V. Conclusion

Analog interference mitigation, as opposed to plain digital solutions, becomes necessary in case the interference starts to limit the receiver's sensitivity due to the limited dynamic range of the analog-to-digital converter (ADC) as, e.g., in the case of co-located jammers or radars and signals intelligence receivers. In this paper, we proposed a method for mitigating narrowband interference in the analog domain by using digitally assisted adaptive filtering and provided experimental results on suppressing such interference in a static laboratory environment. The experimental results show promising performance in terms of interference cancellation and the convergence speed of the adaptive interference canceller over a broad frequency range including the very high frequency (VHF) and ultra high frequency (UHF) bands.

However, the results have also illustrated how phase noise, one of the main performance limiting factors, degrades the interference cancellation efficiency. The presented results are limited to a closed experimental setup in a laboratory environment at moderate transmission powers and require further study to assess the feasibility of co-located analog interference mitigation under realistic channel conditions, mobile scenarios, together with signals of interest, and higher output powers. The proposed interference mitigation method could possibly be extended to work with broadband pseudorandom jamming signals, e.g., in the case of a full-duplex (FD) radio shield, if the narrowband interference reconstruction can be replaced with a pseudorandom interference generator.

References

[1] J. Laster and J. Reed, "Interference rejection in digital wireless communications," *IEEE Signal Processing Magazine*, vol. 14, no. 3, pp. 37–62, May 1997.

[2] P. Ödling, O. P. Börjesson, T. Magesacher, and T. Nordström, "An approach to analog mitigation of RFI," *IEEE Journal on Selected Areas in Communications*, vol. 20, no. 5, pp. 974–986, Jun. 2002.

[3] A. Sabharwal, P. Schniter, D. Guo, D. W. Bliss, S. Rangarajan, and R. Wichman, "In-band full-duplex wireless: Challenges and opportunities," *IEEE Journal on Selected Areas in Communications*, vol. 32, no. 9, pp. 1637–1652, Sep. 2014.

[4] K. Pärlin, T. Riihonen, R. Wichman, and D. Korpi, "Transferring the full-duplex radio technology from wireless networking to defense and security," in *Proc. 52nd Asilomar Conference on Signals, Systems and Computers*, Oct. 2018, pp. 2196–2201.

[5] K. Pärlin, T. Riihonen, and M. Turunen, "Sweep jamming mitigation using adaptive filtering for detecting frequency agile systems," in *Proc. International Conference on Military Communications and Information Systems*, May 2019.

[6] V. Syrjälä, M. Valkama, L. Anttila, T. Riihonen, and D. Korpi, "Analysis of oscillator phase-noise effects on self-interference cancellation in full-duplex OFDM radio transceivers," *IEEE Transactions on Wireless Communications*, vol. 13, no. 6, pp. 2977–2990, Jun. 2014.

[7] D. A. Rich, S. Bo, and F. A. Cassara, "Cochannel FM interference suppression using adaptive notch filters," *IEEE Transactions on Communications*, vol. 42, no. 7, pp. 2384–2389, Jul. 1994.

[8] A. Raghavan, E. Gebara, E. M. Tentzeris, and J. Laskar, "Analysis and design of an interference canceller for collocated radios," *IEEE Transactions on Microwave Theory and Techniques*, vol. 53, no. 11, pp. 3498–3508, Nov. 2005.

[9] S. Ayazian and R. Gharpurey, "Feedforward interference cancellation in radio receiver front-ends," *IEEE Transactions on Circuits and Systems II: Express Briefs*, vol. 54, no. 10, pp. 902–906, Oct. 2007.

[10] D. Korpi, T. Riihonen, V. Syrjälä, L. Anttila, M. Valkama, and R. Wichman, "Full-duplex transceiver system calculations: Analysis of ADC and linearity challenges," *IEEE Transactions on Wireless Communications*, vol. 13, no. 7, pp. 3821–3836, Jul. 2014.

[11] T. Riihonen and R. Wichman, "Analog and digital self-interference cancellation in full-duplex MIMO-OFDM transceivers with limited resolution in A/D conversion," in *Proc. 46th Asilomar Conference on Signals, Systems and Computers*, Nov. 2012, pp. 45–49.

[12] M. Duarte and A. Sabharwal, "Full-duplex wireless communications using off-the-shelf radios: Feasibility and first results," in *Proc. 44th Asilomar Conference on Signals, Systems and Computers*, Nov. 2010, pp. 1558–1562.

[13] S. M. Kuo and D. R. Morgan, "Active noise control: A tutorial review," *Proceedings of the IEEE*, vol. 87, no. 6, pp. 943–973, Jun. 1999.

[14] L. Xu, D. Feng, Y. Liu, X. Pan, and X. Wang, "A three-stage active cancellation method against synthetic aperture radar," *IEEE Sensors Journal*, vol. 15, no. 11, pp. 6173–6178, Nov. 2015.

[15] D. R. Morgan and C. Sanford, "A control theory approach to the stability and transient analysis of the filtered-X LMS adaptive notch filter," *IEEE Transactions on Signal Processing*, vol. 40, no. 9, pp. 2341–2346, 1992.

[16] B. Widrow, J. R. Glover, J. M. McCool, J. Kaunitz, C. S. Williams, R. H. Hearn, J. R. Zeidler, J. E. Dong, and R. C. Goodlin, "Adaptive noise cancelling: Principles and applications," *Proceedings of the IEEE*, vol. 63, no. 12, pp. 1692–1716, Dec. 1975.

[17] A. Sahai, G. Patel, C. Dick, and A. Sabharwal, "On the impact of phase noise on active cancelation in wireless full-duplex," *IEEE Transactions on Vehicular Technology*, vol. 62, no. 9, pp. 4494–4510, Nov. 2013.

[18] E. Ahmed and A. M. Eltawil, "On phase noise suppression in full-duplex systems," *IEEE Transactions on Wireless Communications*, vol. 14, no. 3, pp. 1237–1251, Mar. 2015.